Fizika Nizkikh Temperatur, 2010, v. 36, No. 2, p. 206–211

Superconductivity without dependence on valence electron density in (Al, Zn, Co) doped YBCO systems

Zhang Yufeng

Department of Mathematics and Physics, Shanghai University of Electric Power
28 Xuehai Road, Nanhui District, Shanghai 201300, PRC
E-mail: zyfeng1011@yahoo.com.cn

Wang Dandan and Li Pinglin

School of Physics and Engineering, Zhengzhou University, Zhengzhou 450052, PRC

Received July 30, 2009, revised September 1, 2009

We adopted the x-ray diffraction, oxygen contents, positron annihilation technology and simulation methods to investigate systematically YBa_2Cu_{3-x}(Al, Zn, Co)$_xO_{7-\delta}$ (x = 0–0.5) cuprates. The experimental results and simulated calculations support the existence of cluster effect. Moreover, it is concluded that the cluster effect is an important factor on suppression of the superconductivity and the T_c does not depend directly on the density of valence electron in the samples.

PACS: **68.65.–k** Low-dimensional, mesoscopic, nanoscale and other related systems: structure and nonelectronic properties;
47.54.De Experimental aspects;
47.54.Bd Theoretical aspects.

Keywords: YBCO, simulated calculations, positron annihilation, cluster effect, valence electron.

1. Introduction

The high-T_c cuprates, especially YBCO systems, are still the highlight in the superconducting researches [1–5], however, the microscopic mechanism is challenging harshly to all theories, even as Zaanens statements: «The high-T_c superconductivity is on the list of the most profound physics problems…» [6]. In order to search and comprehend such a problem, scientists suggested many new theories and experimental technologies [7–9], for example, elemental substitution that play an important role in the research of high-T_c cuprates until today [10–13], namely, copper is replaced by magnetic or nonmagnetic elements. According to the traditional theory of magnetic pair-breaking, the nonmagnetic ions doped into superconductors will suppress less the superconductivity than magnetic ions. However, Zn^{2+} doped in YBCO, a kind of nonmagnetic ion, suppresses more forcefully the superconductivity than other nonmagnetic and magnetic ions, like Al and Co. At present, most researchers believe that the superconducting phenomenon occurs on CuO_2 planes [14–16], where Zn^{2+} ions substitute for Cu(2) sites. Hence, Zn doping will suppress noticeably the superconductivity [17,18]. Some scientists suggested Zn doping destroys the background of antiferromagnetism on CuO_2 planes [19]; however, this proposal is still one of viewpoints of magnetic pair-breaking. Besides, what a reason causes the transition temperature T_c to fall faster and faster with the increase of doped concentration [20–25] and so on? Many queries are now still unclear; therefore, further investigations of theories and experiments will be necessary in Al, Zn and Co doped YBCO cuprates.

In order to realize the distribution of doped ions, here we will calculate the total defect energy and average binding energy inside a cluster based on Islam's method [26]. Simulated results reveal the possibility of cluster effect. When the doped concentration increases, the doped ions combine into different clusters on CuO_2 planes and in CuO chains. Afterwards, we use positron annihilation technique (PAT) to probe the change of electron structure as Al, Zn and Co substitute for Cu in YBCO. PAT plays an important role in the investigation of such condensed matters as semiconductors, metal materials and high-T_c cuprates [27–30]. The positron studies examine the properties of normal and superconducting states, such as Fermi surface, O–T transition and the carrier concentration [31–34]. In recent years, Jean and Li et al. reported many important results from positron experiments and theories concerning high-T_c superconducting mechanism [20–24,33–35]. In the present article, we report the systematical investigation concerning

YBa_2Cu_{3-x}(Al, Zn, Co)$_xO_{7-\delta}$ (x = 0–0.5) samples. The theoretic calculations and experimental results of PAT and oxygen content support the existence of cluster effect. Moreover, it is reasoned that cluster effects, as an important factor, suppress the cuprate superconductivity and the T_c variations do not directly depend on the density of valence electron in the samples.

2. Experiments

Samples of YBa_2Cu_{3-x}(Al, Zn, Co)$_xO_{7-\delta}$ (x = 0–0.5) were prepared by the same method as in Refs. 20 and 22–24. Due to the sensitivity of the PAT experiments, all samples were sintered in the same conditions in order to reduce the dispersion of the experimental results. The superconducting transition temperature T_c was measured by the standard dc four-probe method with a voltage resolution of 10^{-7} V (HP3457A). The crystal structures of samples were analyzed by powder x-ray diffraction (XRD) using the D/max-BX-ray diffractometer. The positron lifetime spectra were measured by the ORTEC-100U fast-fast coincidence lifetime spectrometer. Two pieces of identical samples (∅13×3 mm) were sandwiched together with a 10-μC22 Na positron source deposited on a thin Mylar foil (about 1.2 mg/cm^2 thickness). We apply Pilot-U plastic flicker sensor, which was tested by ^{60}Co and showed the excellent time resolution over 220 ps. Each spectrum contains more than $1\cdot10^6$ counts to guarantee the sufficient statistic precision. After subtracting background and source contributions, the lifetime spectra were fitted with two-lifetime components by POSITRON-FIT-EXTENDED program with the best fit (χ^2 =1.0–1.1). The positron lifetime spectra of all samples were measured at the identical environment temperature, (283 ± 1) K, and the results were reproducible.

3. Results and discussions

3.1. Simulated calculations

In order to understand the characteristics of cluster structure, here we perform simulated calculations on the energy minimization principle and framework of Born model, in which the effective pairwise potentials represent the interatomic forces in the following form [26]:

$$\Phi_{ij} = \frac{Z_i Z_j e^2}{4\pi\varepsilon_0 r_{ij}} + A_{ij}\exp\left(-\frac{r_{ij}}{\rho_{ij}}\right) - \frac{C_{ij}}{r_{ij}^6}, \qquad (1)$$

where Φ_{ij} is the effective potentials between ions i and j; Z_i and Z_j are ion valences; r_{ij} is the distance between ions i and j; A_{ij} , C_{ij} and ρ_{ij} are the relative characteristic constants. The first term is the long-range Coulomb interaction; the remaining terms represent the short-range interaction and the shielded revision. Because charge equilibrium determines the ion coordination characteristics in clusters, the clusters should be electrically neutral. The neutral clusters may show several structures, two of which are illustrated as (*a*) and (*b*) on CuO_2 planes in Refs. 20–24. Here (*a*) as Hexamer denotes six doped ions with two common-lateral squares, and (*b*) as Double Square does seven doped ions with two common-apical squares. On CuO_2 planes Cu ions are +2.25 valence, and doped Zn ions are +2, moreover holes exist on oxygen ions [25,36]. These two factors together make electrons lose; consequently, the number of the oxygen ions has to decrease in order to keep the charge equilibrium. For example, in four doped ions cluster, every four Zn^{2+} ions may exclude an oxygen ion, which can be described as $\{4Zn^{2+} \rightarrow 4Cu^{2.25+} - O^{2-}\}$. Nevertheless, one Zn ion alone cannot exclude an oxygen ion. Hence, the binding energy of Zn^{2+} cluster is:

$$E_{\text{bind}} = E_{b1}(4Zn^{2+} \rightarrow 4Cu^{2.25+} - O^{2-}) - \\ - 4E_{b2}(Zn^{2+} \rightarrow Cu^{2.25+}) + E_{b3}(O^{2-}). \qquad (2)$$

where E_{b1}, E_{b2} and E_{b3} are all represented as $E = \sum\Phi_{ij}$. The first term E_{b1} is the cluster total energy, E_{b2} is the binding energy that a Zn^{2+} substitutes for a $Cu^{2.25+}$ ion, and E_{b3} is the binding energy that an O^{2-} ion is lost. For both Hexamer and Double Square, E_{bind} have similar formulation. The average binding energy of every doped ion is $E_{\text{mean}} = E_{\text{bind}}/N$ where N is the number of doped ions in a cluster. Other clusters may likewise be described and calculated. The calculation results are listed in Table 1, in which the negative value of the binding energy indicates the system is bound. As well known, the larger average binding energy is, the more stable a cluster combines. Consequently, the doped ions should prefer to form the cluster with largest average binding energy. It can be concluded from the results listed in Table 1 that doped Al and Co ions prefer to form Hexamer cluster of six ions, while for Zn doping Double Square (a common point, seven ions) clusters have the largest probability. As for the larger cluster, it can be composed by some small clusters, for example, the cluster of eight ions are composed by double four ions and so on.

Table 1. The mean binding energy of per doped ion in the doped YBCO

Cluster	$Al^{3+} - E_m$	$Co^{3+} - E_m$	Cluster	$Zn^{2+} - E_m$
D + O	–2.73	–2.80	D	–1.67
TL + 2O	–2.25	–2.44	TL–O	–1.49
TS + 2O	–2.71	–2.82	TS–O	–1.64
TZ + 2O	–2.10	–2.15	TZ–O	–1.36
H + 3O	–2.83		H–2O	–1.68
H + 4O	–2.85	–3.03	H–O	–1.75
DS + 4O	–2.81	–2.91	DS–2O	–1.78

N o t e s: Here the negative value indicates the binding energy. E_m (eV/ion) is the mean binding energy per doped ion. D + O = Dimmer {2M→2Cu^{2+}+O^{2-}} (M = Al^{3+}, Co^{3+}), «+O» represents an O^{2-} ion is attracted into the cluster;
TL + 2O = Tetramer {4M → 4Cu^{2+} + 2O^{2-}} Linear;
TS + 2O = Tetramer {4M → 4Cu^{2+} + 2O^{2-}} Square;
TZ + 2O = Tetramer {4M → 4Cu^{2+} + 2O^{2-}} Zigzag;
H + 4O = Hexamer {6M → 6Cu^{2+} + 4O^{2-}};
DS + 4O = Double Square {7M → 7Cu^{2+} + 4O^{2-}}.
Besides, Zn^{2+} clusters will squeeze out oxygen ion, which is marked as TL−O and so on. «–O» represents an O^{2-} ion is squeeze out the cluster.

3.2. X-ray diffraction results and cuprate superconductivity

XRD results show that undoped and low-doped Y-123 samples have the well single phase. As doped concentration x increase, samples show slight impure phases at x = = 0.12, x = 0.20 and at x = 0.25 for Zn, Al, and Co doping, respectively. Here in-order three x values correspond with the average binding energy E_m of Zn, Al, and Co. Every cluster in Table 1, namely, x (Zn) < x (Al) < x (Co) has the same relation to E_m(Zn) < E_m(Al) < E_m(Co). Such a result reveals that the small theoretic E_m samples form easily the impure phases in the experiments, so our theoretic calculations are able to reflect the experimental data. All the lattice parameters were calculated by the least square method with powder XRD data, and the results of Zn and Al doped samples are shown in Fig. 1 and Fig. 2. Due to Co doped samples have the similar results to Al doped, the former lattice parameters are not illustrated. For Zn doped samples, the lattice parameter a and b increase slightly with x increasing, because the Zn^{2+} radius (0.74 Å) is larger than the Cu^{2+} radius (0.72 Å), but the O–T transition does not appear in x = 0–0.4. While for Al and Co doping, O–T transition occurs near x = 0.15 and 0.12, respectively.

Generally, O–T transition results from the change of oxygen content in Cu–O chains [20–23]. Thus the variation of lattice parameters a and b indicates that Al and Co ions enter mainly Cu(1) sites, which is consistent with Hoffmann et al. experiments [37,38]. It should be noticed that O–T transition occurs before the appearance of impure phases, which reflects the intrinsic properties of Al and Co doped Y123 systems. For the same reason, the variation of lattice parameters shows that Zn ions enter mainly Cu(2) sites on CuO_2 planes [39,41], where the superconductivity occurs. It implies that the superconductivity suppressed by Zn doping should be stronger than by Al and Co doping. In our experiments [20,22–24] , the T_c is 92 K for Y123 compounds without elemental substitution, which call undoped

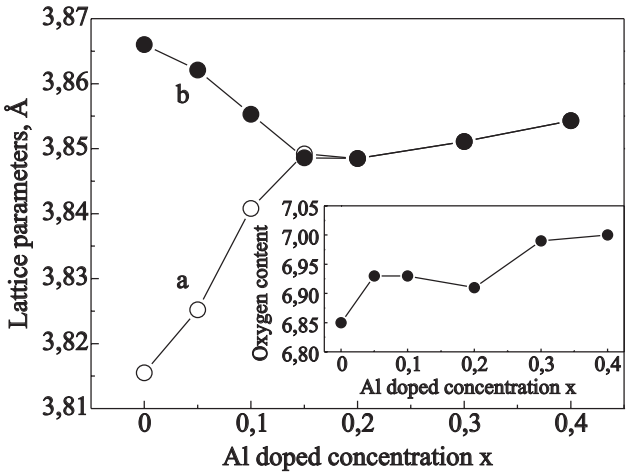

Fig. 1. Lattice parameter a and b variation with Al doped concentration x in YBCO systems. The insert picture indicates the oxygen content variation with x (Ref. 17).

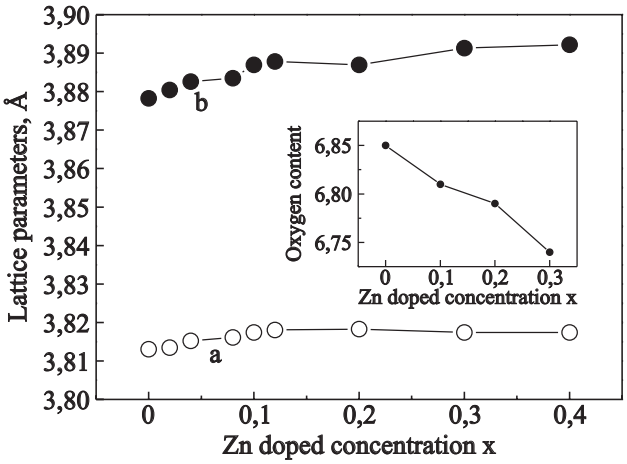

Fig. 2. Lattice parameter a and b variation with Zn doped concentration x in YBCO systems. The insert picture indicates the oxygen content variation with x (Ref. 17).

samples in the text. For Al doping, during x = 0–0.10, the T_c falls slightly to 91 K; at x = 0.20, the T_c is 83.2 K; and at x = 0.40, T_c = 42.5 K. And the T_c falls to about 72.3 K for Zn concentration x = 0.10; when x = 0.20, the T_c is 42.6 K and for x = 0.40, T_c = 15.7 K. While for Co doped samples, the T_c decreases stepwise with x increasing, when x = 0.05, the T_c is about 80.0 K; at x = 0.10, the T_c is 67.5 K; at x = 0.20, the T_c is 44.5 K; and if x = 0.30, one has T_c = 21.0 K. Obviously, when x < 0.20, Zn doping suppresses the superconductivity much more severely than Al and Co doping, however, when x > 0.20, Co doping suppresses most strongly the superconductivity in the three doped ions. It suggests that the cluster effect is still an important factor in suppression of the superconductivity because Co ions show the strongest cluster effect as above calculation results.

3.3. Oxygen content variations

The insert picture in Fig. 1 and Fig. 2 show the experimental results of oxygen content concerning Al and Zn doped samples [17]. Here the oxygen content of Co doping is omitted as being similar to Al doping. For M^{3+} (Al^{3+}, Co^{3+}) doping, M^{3+} valence is higher than Cu^{2+} in Cu–O chains, the dispersed ions cannot capture one oxygen ion due to charge equilibrium. As x increases the ions form clusters, which are able to capture oxygen ions, so the oxygen content should rise in Al and Co doped samples. However, for Zn doping, the oxygen content falls obviously with x increase, such variation characteristics are consistent with the simulated calculations, because Zn^{2+} valence is lower than $Cu^{2.25+}$ and the dispersed ions cannot extrude oxygen ions to achieve electric neutrality. While the cluster has not formed yet and Zn ions are distributed randomly, there are hardly oxygen vacancies around Zn ions and the oxygen content should not decrease. With x increasing, Zn ions form more and more clusters, because Zn ions require less oxygen ions for coordination than Cu,

the extra oxygen ions will be extruded from the clusters. Therefore, oxygen vacancies would appear on CuO_2 planes, and then the oxygen content should descend noticeably (Fig. 2, insert). We can conclude that cluster effect is indeed a factor that causes oxygen content to reduce in Zn doped YBCO. From the above analysis, oxygen content variation characteristics in those doped samples can be explained convincingly by the cluster effect. In fact, the PAT experiments have the same conclusions.

3.4. Positron experiments

PAT experiments are described in detail in our other papers [20–24]. The positron lifetime is defined as the inverse of annihilation rate. According to the model of two-state capture in condensed matter [42] with the short lifetime τ_1 and the long lifetime τ_2 , the processes of positron annihilation are attributed to free-state annihilation and trapping-state annihilation, respectively. The former intensity I_1 denotes the proportion of free-state annihilation to total annihilation events, the latter intensity $I_2 = 1 - I_1$. τ_1 reflects mainly the annihilation process in the perfect crystal lattices and can be used to detect the electron distribution of the inner microstructure. τ_2 reflects mainly the process of positron captured in the imperfect areas inside the materials; it can characterize the intrinsic structure and preparation quality of samples. If positrons annihilate in the imperfections, such as oxygen vacancy, twin boundary, dislocation, and cation vacancies, τ_2 will be larger, sometimes it is noted as τ_3, generally $\tau_3 > 800$ ps [43–45]. Our samples do not contain τ_3 component, this indicates the credibility of the sample quality.

According to the characteristics of positron annihilation, local electron density $n_e = 1/(\pi r_0^2 c\tau_{\text{bulk}})$, where r_0 is the classical electron radius, c is the velocity of light, and τ_{bulk} is the systematical lifetime parameter, it is defined as:

$$1/\tau_{\text{bulk}} = I_1/\tau_1 + I_2/\tau_2 . \qquad (3)$$

Some relational calculation results [46,47] show that about 90% positrons annihilate with the valence electrons, and only about 10% positrons annihilate with the electrons within the atomic kernel. These results indicate that the n_e amount is determined mainly by the valence electrons, so we may regard the density of valence electron as the n_e without influence on the general conclusions.

When M^{+3} (Al^{+3}, Co^{+3}) enter Cu–O chains as above, the dispersive M^{+3} contains one valence electron less than Cu^{2+}, so the n_e should drop. However, the doped ions form clusters as x increases, oxygen ions will be attracted into the crystal lattice. Once introduced by the clusters, every oxygen ion will attract two valence electrons in terms of charge equilibrium. Therefore the valence electron density rises, namely, the n_e shows a rising trend. When the n_e dropping and rising reach a balance, the low saturation emerges as shown in the experiments [24]. Obviously, such a result originates from the cluster effect. In contrast, while +2 valence ions enter CuO_2 planes, Zn^{2+} loses fewer electrons than $Cu^{2.25+}$, so the density should rise on the consideration of valence state. However, as x increase, the Zn ions start to form clusters. As mentioned before, every four Zn^{2+} will extrude an O^- (including a hole) which carries away two valance electrons, so the density begin to fall. When the rising and falling of the density reach a balance, the density n_e tends to high saturation [20], which is influenced evidently by the cluster effect. As a result, the n_e saturation also can be elucidated satisfactorily through the cluster effect as the oxygen content variations above.

3.5. Valence electron density and the T_c of cuprates

Figure 3 shows the relationship between the T_c and the reduced n_e in Al, Zn and Co doped samples. For Al and Co doped samples, both reduced n_e have the great decrease in the little doping, the T_c descends only slightly, especially in the Al doped samples, but the reduced n_e of Co doped samples descends faster than that of Al doped in the same concentration x, as shown in the figure, so the n_e–T_c curve turning point in Co doped samples is further from $n_e = 1.00$ than that in Al doped, such a result still gives evidence that the E_m is larger in Co doped samples. Below the curve turning point in both samples, the T_c seems to lose further the association with the reduced density n_e, in particular, when both T_c drop sharply, the reduced n_e varies only slightly. In fact, when x is low, both ions enter the crystal lattice in individual, M^{3+} loses more valence electrons than Cu^{2+}, so the density n_e will decrease. However, the T_c descends slightly with the density change because the dispersed ions cannot destroy the crystal lattice. Below the curve turning point the T_c starts to drop sharply with clusters appearing. On our idea, the stronger cluster effect is, the stronger it will distort the structure of crystal lattice. So the superconductivity is seriously suppressed in both samples. In contrast with both above, the n_e–T_c curve of Zn doping has the opposite variation trend in the beginning stage, though the reduced density raises greatly, the T_c descends still slightly, below the curve turning point the T_c

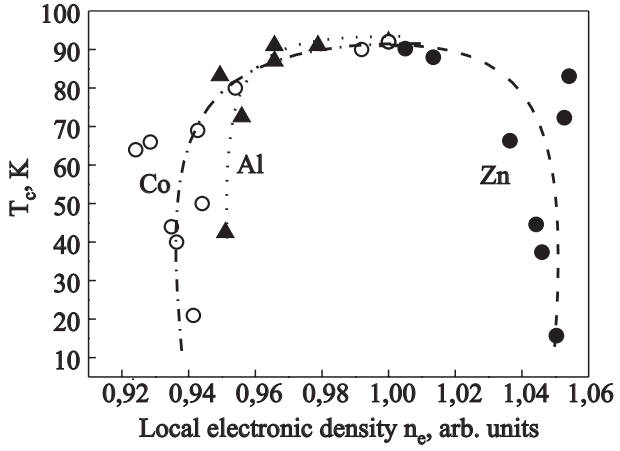

Fig. 3. The variation of superconducting transition temperature T_c with reduced valence electron density n_e in Al, Zn and Co doped YBCO systems.

starts to drop sharply from 72.3 K to 15.7 K, whereas the reduced n_e increases only slightly. As above statements, similarly, when x is small, Zn ions enter the crystal lattice in individual; Zn^{2+} loses fewer electrons than $Cu^{2.25+}$, so the density will increase. However, the T_c descends slightly with the density increasing, because the dispersed ions do not destroy the crystal lattice. While the Zn clusters appear in the doped samples, the structures of crystal lattice will be distorted by the cluster effect, which will influence directly the pairing and transportation of carriers, and thus the superconductivity is suppressed markedly, then the T_c starts to drop sharply. Anyway, when the reduced density increases or decreases essentially, the T_c alters only slightly; on a contrary, while the T_c falls dramatically, the reduced density changes hardly. As a result, we can conclude that the T_c has no direct connection with the valence electron density. However, when the cluster effect strengthens in the region of turning point, the T_c falls noticeably. Therefore, the cluster effect is an important factor that suppresses the cuprate superconductivity.

4. Conclusions

In conclusion, the high-T_c cuprates $YBa_2Cu_{3-x}(Al,Zn,Co)_xO_{7-\delta}$ (x = 0–0.5) have been analyzed and studied systematically by XRD, positron annihilation technique, oxygen content, and calculations of binding energy. The simulated calculations, the variations of oxygen content and positron experiments support congruously the existence of cluster effect. Especially, it is reasoned that the cluster effect is an important factor in suppression of high-T_c cuprate superconductivity and the T_c has no direct connection with the density of valence electron.

This work is supported by The Natural Science Foundation of China (No.10647145).

1. U. Schwingenschlogl and C. Schuster, *Phys. Rev.* **B79**, 092505 (2009).
2. H. Yamase, *Phys. Rev.* **B79**, 052501 (2009).
3. X. Wang, A. Dibos, and J.Z. Wu, *Phys. Rev.* **B77**, 144525 (2008).
4. H.H. Song, M.W. Davidson, and J. Schwartz, *Supercond. Sci. Tech.* **22**, 062001 (2009).
5. W. Markowitsch, W. Lang, J.D. Pedarnig, and D. Bauerle, *Supercond. Sci. Tech.* **22**, 034011 (2009).
6. J. Zaanens and T. Senthil, *Nature Phys.* **2**,138 (2006).
7. J. Guo, C. Dong, H. Gao, H.H. Wen, L.H. Yang, F. Zeng, and H. Chen, *Chin. Phys.* **B17**, 1124 (2008).
8. C. Dong, *Chin. Phys.* **B15**, 3005 (2006).
9. L.B. Shi, Y. Zheng, J.Y. Ren, M.B. Li, and G.H. Zhang, *Acta Phys. Sin.* **57**, 1183 (2008).
10. Y. Fukuuzumi, K. Mizuhaohi, K. Takenaka, and S. Uchida, *Phys. Rev. Lett.* **76**, 684 (1996).
11. H. Salamati and M. Mohammadi, *J. Phys. IV France* **123**, 19 (2005).
12. B.Nachumi, A. Keren, K. Kojima, M. Larkin, G.M. Luke, O. Tcheryshov, Y.J. Uemura, N. Ichikawa, M. Goto, and S. Uchida, *Phys. Rev. Lett.* **77**, 5421 (1996).
13. Y.K. Kuo, C.W. Schneider, M.J. Skove, M.V. Nevitt, G.X. Tessema, and J.J. Mcgee, *Phys. Rev.* **B56**, 6201 (1997).
14. H. Takagi, *Physica* **C341-348**, 3 (2000).
15. A.H. Macdonald, *Nature* **414**, 409 (2001).
16. M. Capone, M. Fabrizio, C. Castellani, and E. Tosatti, *Science* **296**, 2364 (2002).
17. M. Tarascon, P. Barboux, P.F. Miceli, L.H. Greene, G.W. Hull, M. Eibschutz, and S.A. Sunshine, *Phys. Rev.* **B37**, 7458 (1988).
18. R.S. Horland and T.H. Geballe, *Phys. Rev.* **B39**, 9017 (1989).
19. J. Axnäs, W. Holm, Yu. Eltsev, and Ö. Rapp, *Phys. Rev.* **B53**, 3003 (1996).
20. P.L. Li, J.C. Zhang, G.X. Cao, C. Jing, and S.X. Cao, *Phys. Rev.* **B69**, 224517 (2004).
21. P.L. Li, J.C. Zhang, G.X. Cao, D.M. Deng, L.H. Liu, C. Dong, C. Jing, and S.X. Cao, *Acta Phys. Sin.* **53**, 1223 (2004).
22. A.H. Wang, X.X. Wang, S.F. Li, J. Zhang, H.Q. Lu, L.M. Gao, X.L. Li, Y.Y. Wang, and P.L. Li, *J. Low Temp. Phys.* **149**, 89 (2007).
23. P.L. Li, Y.Y. Wang, Y.T. Tian, J. Wang, X.L. Niu, J.X. Wang, D.D. Wang, and X.X. Wang, *Chin. Phys.* **B17**, 3483 (2008).
24. A.H. Wang, X.X. Wang, Y.G. Cao, X.L. Li, Y.Y. Wang, L.M. Gao, H.Q. Lu, J. Zhang, and P.L. Li, *Fiz. Nizk. Temp.* **34**, 219 (2008) [*Low Temp. Phys*. **34**, 168 (2008)].
25. R.P. Gupta and M. Gupta, *Physica* **C305**, 179 (1998).
26. M.S. Islam and C. Aanathamohan, *Phys. Rev.* **B44**, 9492 (1991).
27. K. Saarinen, J. Niddils, H. Kauppinen, M. Hakala, M.J. Puska, P. Hautojarvi, and C. Corbel, *Phys. Rev. Lett.* **82**, 1883 (1999).
28. A.I. Kul'menrt'ev, *Eur. Phys. J. Appl. Phys*. **25**, 191 (2004).
29. T.E. M. Staab, M. Haugk, Th. Frauenheim, and H.S. Leipner, *Phys. Rev. Lett.* **83**, 5519 (1999).
30. A. Somoza, A. Dupasquier, I.J. Polmear, P. Folegati, and R. Ferragut, *Phys. Rev.* **B61**, 14454 (2000).
31. T. Banerjee, R.N. Viswanath, D. Kanjilal, R. Kumar, and S. Ramasamy, *Solid State Commun*. **114**, 655 (2000).
32. D. Udayan, D. Sanyal, S. Chauahuri, P.M. G. Nambissan, T. Wolf, and H. Wuhl, *Phys. Rev.* **B62**, 14519 (2000).
33. Y.C. Jean, J. Kyle, H. Nakanishi, and P.E.A. Turchi, *Phys. Rev. Lett*. **60**, 1069 (1988).
34. J.C. Zhang, F.Q. Liu, and G.S. Cheng, *Phys. Rev.* **A201**, 70 (1995).
35. J.C. Zhang, L.H. Liu, C. Dong, J.Q. Li, H. Chen, X.G. Li, and G.S. Cheng, *Phys. Rev.* **B65**, 054513 (2002).
36. P.C. Li, H.S. Yang, Z.Q. Li, Y.S. Chai, and L.Z. Cao, *Chin. Phys*. **11**, 285 (2002).
37. J.F. Bringley, T.M. Chen, B.A. Averill, K.M. Wong, and S.J. Poon, *Phys. Rev.* **B38**, 2432 (1988).
38. L. Hoffmann, A.A. Manuel, M. Peter, E. Walker, M. Gauthier, A. Shukla, B. Barbiellini, S. Massidda, Gh. Adam,

W.N. Hardy, and R.X. Liang, *Phys. Rev. Lett.* **71**, 4047 (1993).
39. J.M. Tarascon, L.H. Greene, P. Barboux, W.R. McKinnon, G.W. Hull, T.P. Orlando, K.A. Delin, S. Foner, and E.J. McNiff, Jr., *Phys. Rev.* **B36**, 8393 (1987).
40. G. Xiao, M.Z. Cieplak, and C.L. Chien, *Phys. Rev*. **B42**, 240 (1990).
41. N. Bulut, D. Hone, D.J. Scalapino, and E.Y. Loh, *Phys. Rev. Lett.* **62**, 2192 (1989).
42. P. Haotuojiawei, *Positron-Annihilation Technology*, Science Press (1983), p. 255.
43. C. Nagel, K. Ratzke, E. Schmidtke, F. Faupel, and W. Ulfert*, Phys. Rev.* **B60**, 9212 (1999).
44. A. Somoza, A. Dupasquier, I.J. Polmear, P. Folegati, and R. Ferragut*, Phys. Rev.* **B61**, 14454 (2000).
45. L.J. Li, Z.X. Wang, and J.L. Wu, *Acta Phys. Sin.* **47**, 844 (1998).
46. K.O. Jensen, R.M. Nieminen, and M.J. Puaka, *J. Phys. Cond. Matter* **1**, 3727 (1989).
47. H.B. Zhang and H. Sato, *Phys. Rev. Lett.* **70**, 1697 (1993).